

# Selective Depletion Interactions in Mixtures of Rough and Smooth Silica Spheres

Marlous Kamp,<sup>†</sup> Michiel Hermes,<sup>†</sup> Carlos M. van Kats,<sup>†</sup> Daniela J. Kraft,<sup>‡</sup> Willem K. Kegel,<sup>§</sup> Marjolein Dijkstra,<sup>\*,†</sup> and Alfons van Blaaderen<sup>\*,†</sup>

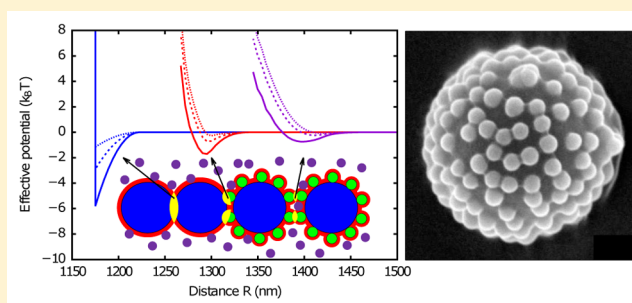
<sup>†</sup>Soft Condensed Matter, Debye Institute for Nanomaterials Science, Utrecht University, Princetonplein 1, 3584 CC Utrecht, The Netherlands

<sup>‡</sup>Soft Matter Physics, Huygens-Kamerlingh Onnes Lab, Leiden University, Niels Bohrweg 2, 2333 CA Leiden, The Netherlands

<sup>§</sup>Van 't Hoff Laboratory for Physical & Colloid Chemistry, Debye Institute for Nanomaterials Science, Utrecht University, Padualaan 8, 3584 CH Utrecht, The Netherlands

## S Supporting Information

**ABSTRACT:** The depletion interaction as induced between colloids by the addition of a polymer depletant is one of the few ways in which short-ranged attractions between particles can be controlled. Due to these tunable interactions, colloid–polymer mixtures have contributed to a better understanding of the role of attractions both in equilibrium phenomena such as phase transitions and liquid surfaces as well as in systems out of equilibrium such as gelation and the glass transition. It is known that, by simple geometric effects, surface roughness decreases the strength of the depletion interaction. In this study, we demonstrate both by Monte Carlo simulations and experiments that it is possible to generate enough difference in attraction strength to induce phase separation in smooth particles but not in rough particles. Roughness was induced by coating smooth particles with smaller spherical colloids. We indicate how effective potentials can be obtained through simulations and how the interplay between gravity and the depletion interaction with a flat container wall can be used to obtain a simple measure of the interaction strengths as a function of roughness.



## INTRODUCTION

In recent decades, the number of colloidal model systems with ever more complex shapes has strongly increased.<sup>1–4</sup> However, for effective control over the self-assembly, phase behavior, and other properties of such systems, not only the particle shape but also other aspects of the interparticle interactions need to be controlled. In this paper, we focus on one of the few ways attractions can be induced between colloidal particles in a controlled way, namely by polymer induced depletion interactions. Depletion attractions are the result of an imbalance of the osmotic pressure induced by a small polymer or other colloid—the depletant—when two larger colloidal particles get closer to each other than the diameter of the depletants (see Figure 1 and refs 5–10.). For relatively low concentrations of the bigger colloids and the depletion agent, the attraction strength is proportional to the concentration of the depletant and the overlap volumes in which the depletant cannot penetrate. As indicated schematically in Figure 1 and as has been demonstrated recently in several papers (see e.g. refs 11 and 12) the depletion interaction can be significantly reduced if surface roughness is introduced with a size on the order of the depletant size. These ideas are more recent extensions of the realization that geometry can be used to affect the overlap volumes.<sup>13</sup> Recent beautiful examples of manipulat-

ing overlap volumes are the lock-and-key interactions between convex and concave particles<sup>14</sup> and (asymmetric) dumbbell-shaped particles that formed colloidal micellar aggregates,<sup>15</sup> and a reversible crystal structure switch by changing the size of the depletant in situ.<sup>16</sup> In the case of the asymmetric dumbbell-shaped particles, local roughness (on one of the particle lobes) and the anisotropic shape of the dumbbell particle both play a role and give rise to complex phase behavior. In this paper, we focus our attention on mixtures of rough and smooth spheres of approximately the same size. This system is simpler than that presented in previous work, as the particle shapes are all convex only. It is in some sense also a limiting case, as it is clear from inspecting Figure 1 that depletion zones between spheres are relatively small and would be significantly increased if the surfaces were more flat like in the experiments from refs 11 and 12, and/or had also concave parts.<sup>14,17</sup> The question that we set out to answer in this paper is whether it is possible in mixtures of rough and smooth spheres to induce strong enough attractions between the smooth spheres that they would phase separate or gel while the interactions between a smooth

Received: October 30, 2015

Revised: January 6, 2016

Published: January 8, 2016

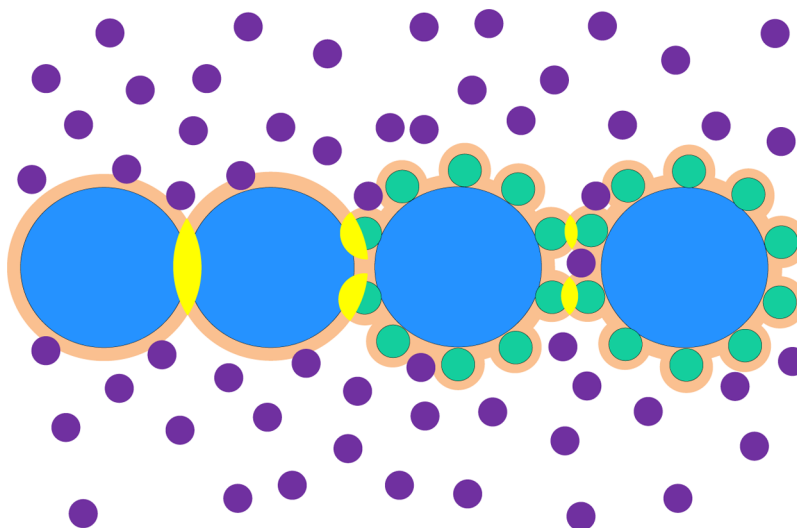


**Figure 1.** Depletion zones (light salmon) and overlap volumes (yellow) for two smooth spheres; a rough and a smooth sphere; and two rough spheres. Colloids are depicted in blue, small spheres that form roughness in green, and depletant in purple.

and rough particle (and thus also between two rough spheres) stay below that necessary to induce phase separation. Interestingly, the answer is yes, which is illustrated by confocal microscopy real-space measurements of mixture of rough and smooth sphere for which a depletion interaction induced by polymer resulted in the formation of a gel between the smooth particles while the dynamics of the rough particles labeled with a different dye remained still completely diffusive in between the gelled phase.

It is clear that specifics of the interactions depend on many parameters such as the screening length of the solvent; the concentration of depletant; and the size of the particles with respect to both the size of the depletant and the surface roughness of the colloids. Therefore, we also demonstrate a simple experimental procedure—that was validated by our simulations—to gauge the strength of the interactions. In this procedure, we used a competition between the depletion attractions and gravity. We determined at what depletant volume fractions the larger particles with different smoothness remained attracted against gravity onto a flat wall oriented perpendicular to gravity. Roughness on the particles was controlled by aggregating a layer of smaller silica spheres of opposite charge on top of smooth silica spheres. Using differently fluorescently labeled components allowed efficient characterization by real space confocal measurements. The effect of varying several of the many variables that influence the effective interactions was studied by simulations in order to assess their importance.

In the following, we first explain the experimental and simulation methods used. Subsequently, we describe and discuss both the effective depletion interaction potentials and how they are influenced by several variables obtained from the simulations and the experiments performed to measure the interaction strength and induce the phase separation/gelation.

## METHODS

**Simulation Details. Model and Effective Interactions.** The rough colloidal particles are modeled as hard spheres with diameter  $\sigma_c$  coated with small hard spheres of diameter  $\sigma_r$  on the colloidal surface acting as roughness. The smooth particles are modeled as hard spheres of diameter  $\sigma_s$ . We consider  $N_c$  coated particles at positions  $\vec{R}_i$  with orientations  $\hat{\omega}_i$  in a macroscopic volume  $V$  at temperature  $T$ . As a

depletant,  $N_p$  polymers are placed at positions  $\vec{r}_j$  in this volume. The polymer diameter  $\sigma_p$  is taken to be twice the radius of gyration  $R_g$  ( $\sigma_p = 2R_g$ ). The colloid and polymer interactions are described by a pairwise colloid–colloid interaction Hamiltonian  $H_{cc} = \sum_{i < j} \phi_{cc}(\vec{R}_{ij}, \hat{\omega}_i, \hat{\omega}_j)$ , a pairwise colloid–polymer Hamiltonian  $H_{cp} = \sum_{i=1}^{N_c} \sum_{j=1}^{N_p} \phi_{cp}(\vec{R}_i - \vec{r}_j, \hat{\omega}_i)$ , and a polymer–polymer Hamiltonian  $H_{pp} \equiv 0$  as the polymers are assumed to be ideal. Here we introduced the colloid–colloid pair potential  $\phi_{cc}$  and the colloid–polymer pair potential  $\phi_{cp}$  given by the following:

$$\beta\phi_{cc}(\vec{R}_{ij}, \hat{\omega}_i, \hat{\omega}_j) = \begin{cases} \infty & \text{for } (\xi(\vec{R}_{ij}, \hat{\omega}_i, \hat{\omega}_j) < 0), \\ 0 & \text{otherwise,} \end{cases} \quad (1)$$

$$\beta\phi_{cp}(\vec{R}_i - \vec{r}_j, \hat{\omega}_i) = \begin{cases} \infty & \text{for } (\xi(\vec{R}_i - \vec{r}_j, \hat{\omega}_i) < 0), \\ 0 & \text{otherwise,} \end{cases} \quad (2)$$

with  $\beta = (k_B T)^{-1}$  with  $k_B$  the Boltzmann constant, and where  $\vec{R}_{ij} = \vec{R}_i - \vec{R}_j$ ,  $\xi(\vec{R}_{ij}, \hat{\omega}_i, \hat{\omega}_j)$  denotes the surface-to-surface distance between two coated particles, and  $\xi(\vec{R}_i - \vec{r}_j, \hat{\omega}_i)$  is the surface-to-surface distance between a coated particle and a polymer coil. The total interaction Hamiltonian of the system reads  $H = H_{cc} + H_{cp}$ . The kinetic energy of the polymers and the colloids is not considered here explicitly, as it is trivially accounted for in the classical partition sums to be evaluated below.

The binary mixture of coated particles and ideal polymers with interaction Hamiltonian  $H$  can be mapped onto an effective one-component system with Hamiltonian  $H_{\text{eff}}$  by integrating out the degrees of freedom of the polymer coils. The derivation follows closely those of refs 18–22., see SI. The effective Hamiltonian of the coated particles is written as follows:

$$H_{\text{eff}} = H_{cc} - z_p V_f, \quad (3)$$

where  $z_p V_f = z_p V_f(R, \hat{\omega})$  is the negative of the grand potential of the fluid of ideal polymer coils in the static configuration of  $N_c$  coated colloids with coordinates  $\vec{R}$  and orientations  $\hat{\omega}$ . Here  $V_f(R, \hat{\omega})$  is the free volume of the polymers in the configuration of the colloids. The orientation-averaged effective pair potential reads as follows:

$$\beta\phi_{\text{eff}}(R_{ij}) = -\log\left(\frac{1}{16\pi^2} \int_{\Omega} d\hat{\omega}_i \int_{\Omega} d\hat{\omega}_j \exp[-\beta\phi_{cc}(\vec{R}_{ij}, \hat{\omega}_i, \hat{\omega}_j)] - z_p \int_V d\vec{r} f(\vec{R}_i - \vec{r}, \hat{\omega}_i) f(\vec{R}_j - \vec{r}, \hat{\omega}_j)\right). \quad (4)$$

Since the integrals over the orientations of the particles cannot be solved directly, we perform the orientation average by evaluating the integrand for many different random orientations. We have checked the convergence of the integrations.

**Generation of Model Rough Particles.** Rough particles similar to those used in the experiments were modeled by Monte Carlo (MC) simulations of a binary mixture of oppositely charged particles in the NVT ensemble. We assume the particles interact via Yukawa potentials with Debye length  $\kappa^{-1}$ : we choose a positive charge on the large colloids with diameter  $\sigma_c$  and negative charge on the small particles with diameter  $\sigma_r$ . The simulation is run, and the charge of the large colloids increased until all the small spheres have aggregated onto the large spheres. We take the end configuration of such a simulation as a model for a rough particle. The structure of the small particles on the surface of the large colloids can be tuned by the choice of  $\kappa\sigma_c$ .

**Calculations of Pair Potentials and Overlap Volumes.** We calculate the pair potentials between two rough particles, two smooth particles or a rough and a smooth particle in the following manner. Two such particles are placed in a cubic simulation box, and we sample  $1 \times 10^5$  random orientations of the two particles. For the first 1000 nonoverlapping configurations, we calculate the pair potential. If nonoverlapping configurations are found, then the particles are moved closer together and we generate orientations and calculate the potential again.

To calculate the overlap volume, we divide the simulation box containing the two particles into smaller cells. Cells which are not completely inside or completely outside the overlap volume are divided into eight subcells. For each subcell, the procedure is repeated until the volume of the cell is smaller than  $1 \times 10^{-5}$ . Then ten randomly distributed points are generated in these subcells to estimate the overlap volume in this cell. The final overlap volume is the sum of the overlap volume of all cells. In a test for a specific configuration the difference between the analytic expression and the computer-generated result was less than  $1 \times 10^{-5}\sigma^3$ .

**Experimental Section. Particle Synthesis.** Rough and smooth particles were synthesized as described in the SI, combining elements of ref 17 and refs 23–26. Briefly, for the rough particles, we synthesized  $1.18 \pm 0.01 \mu\text{m}$  (polydispersity 2%) silica particles following a Stöber routine. These silica colloids were given a positive charge by adsorption of PAH molecules. Subsequently, the silica cores were decorated with small particles by slow sedimentation of the positively charged core colloids through a dispersion of small  $130 \pm 4 \text{ nm}$  negatively charged silica particles. Finally, a thin layer of Stöber silica was grown onto these colloids, and they were functionalized with 3-methacryloxypropyltrimethoxysilane (MPS) for dispersion in the index-matching solvent cyclohexyl chloride (CHC) through the adsorption of a steric stabilizer (poly[12-hydroxystearic acid] (PHSA) comb-grafted onto a poly[methyl methacrylate] (PMMA) backbone).

**Interaction Strength and Phase Separation Experiments.** A CHC stock solution was prepared with a stabilizer concentration of 0.6 g/L and saturated with tetrabutyl ammonium chloride (TBAC). The salt and the stabilizer were added to the CHC before the colloids were dispersed in it. The steric stabilizer can act as an extra depletion agent, but at the concentration used both rough and smooth particles did not aggregate without adding an extra polymer depletant. A DLS measurement (on a ZetaSizer Nano, Malvern Instruments) of 2 wt % PS (polystyrene) in the CHC stock solution indicated a (hydrodynamic) radius of gyration of the polymer in this solution of  $23 \pm 1 \text{ nm}$ .

The Debye screening length  $\lambda_D$  in an electrolyte solution is given by the following:<sup>27</sup>

$$\lambda_D = \sqrt{\frac{\epsilon\epsilon_0 k_B T}{2e^2 N_A I}} \quad (5)$$

with  $\epsilon$  the dielectric constant of the medium,  $\epsilon_0$  the vacuum permittivity,  $k_B$  the Boltzmann constant,  $T$  the absolute temperature,  $e$  the elementary charge,  $N_A$  Avogadro's number, and  $I$  the ionic strength. The added amount of TBAC was equivalent to 2 mM, yet

not all TBAC was expected to dissociate. The conductivity of the solution was  $0.441 \pm 0.003 \mu\text{S/cm}$ ; with Walden's rule one arrives at a Debye length of  $41.3 \pm 0.2 \text{ nm}$ .

PS (565.500 g/mol) dispersions were prepared from this stock solution, with concentrations of 3–8 g/L (3–8 wt %). Additionally, stock dispersion of colloids were prepared: a stock dispersion of the smooth colloids with a concentration of 70 g/L, and a stock dispersion of the rough colloids with the same concentration. For phase separation experiments, samples with both smooth and rough particles were obtained by adding together equal volumes of the two stock dispersions. Samples with depletant were obtained by adding an equal volume of polymer stock solution to a volume of such a mixed dispersion. Capillaries were filled by dipping them into the dispersion and sealed with UV glue (Norland Optical Adhesive 68). After curing of the glue, capillaries were sonicated for a few seconds to liberate particles potentially sticking to the walls by depletion interaction. Afterward, some capillaries were stored in a rotating stage<sup>28</sup> to approximately average out the effects of gravity. Samples were examined by confocal scanning laser microscopy (Leica SP2 microscope, horizontal stage, equipped with a 63x lens and Leica type F immersion liquid).

For experiments to estimate the interaction strength, dispersions were prepared as follows. Equal volumes were prepared, of which 50% consisted of the stock solution of either rough or smooth spheres in CHC, and 50% consisted of polymer stock solution diluted with CHC stock solution (in a volume ratio depending on the desired final polystyrene concentration). Capillaries were filled with these dispersions, sealed with UV-glue, and left on one side for 30 min. The capillaries were then turned upside down and imaged by confocal microscopy. After 30 min equilibration time, the capillaries were observed again; this time was adequate to allow particles not fixed to the (now top) wall by depletion attraction to sediment. At four locations in the capillary, an confocal image was obtained from the particles stuck to the top capillary wall and the particles that had sedimented to the bottom wall. Interactive Data Language (IDL) tracking software by Crocker, Grier, and Weeks<sup>29</sup> was used to count the number of particles on each frame. The ratio of particles sticking to the top wall to the total number of particles was calculated for each location. These fractions were averaged for the four locations to obtain the average fraction of particles sticking to the top wall.

## RESULTS AND DISCUSSION

**Simulations: Effect of Surface Coverage on the Effective Depletion Potential.** Effective pair potentials were calculated for two colloids of radius  $\sigma_c$  covered with small particles of radius  $\sigma_r = 0.15\sigma_c$  and polymers with a reservoir packing fraction of 0.16. The surface coverage was varied from 0 to 300 small particles per large particle. The potentials are summarized in Figure 2. The line for zero surface coverage shows that the attraction minimum for smooth particles is at  $-6 k_B T$ . For a sparse surface coverage of 25 particles, the potential has two minima: one at  $R = \sigma_c$  and one at  $R = \sigma_c + \sigma_r$ . Upon increasing the surface coverage to 100–150 small particles per large particle, a single minimum develops at  $R = 1.28\sigma_c$  as the first layer of particles becomes denser. When the first outer layer is complete (we deduce that this occurs at approximately  $1.7 \times 10^2$  small particles), the minimum starts to shift to higher values and it reaches  $R = 1.5 \sigma_c$  for a full second layer (around  $3.3 \times 10^2$  small particles). All in all, the best reduction of the attractive depletion potential is reached when the outer layer is incomplete, in this case when the surface packs 60–80 or 220–260 small particles, and not when the outer layer is complete at around  $1.7 \times 10^2$  or  $3.3 \times 10^2$  particles. For this reason, experiments were conducted with particles with an incomplete surface packing.

The range of attraction is increased by the rough surface. It is equal to  $\sigma_p$  for smooth particles. For rough spheres, the range is

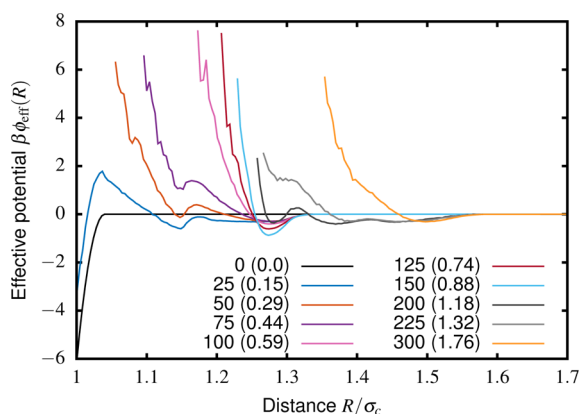


**Figure 2.** Effective depletion potentials as a function of interparticle distance for two rough particles, shown for increasing numbers of small particles decorating the surface. The first number in the legend denotes the number of small spheres, while the second label (in brackets) indicates the fraction of one complete layer. The bare spheres have a diameter  $\sigma_c$ . The polymer has a diameter of  $0.04\sigma_c$  and a polymer reservoir packing fraction of  $\eta_p^r = 0.16$ . The small spheres have a diameter of  $0.15\sigma_c$ . The attraction between the smooth spheres is  $6 k_B T$ .

about  $\sigma_p + \sigma_r$  at complete coverage for sufficiently high polymer fugacity. The extension of the range is even more pronounced for incompletely covered particles. The random nature of the aggregation process makes it very unlikely that two particles will have a commensurate surface roughness. Due to the scarcity of these configurations, the loss in rotational entropy is large. For the polymer concentrations studied here, the rough particles are always less attractive than the smooth particles as a result of this loss in entropy. At very high polymer concentrations, the loss of rotational entropy will no longer be significant and some of the rough particles will become more attractive than the smooth particles due to the larger overlap volume possible between commensurate surfaces. For the parameters studied here, we only observed this for polymer volume fractions much larger than one.

**Simulations: Effect of Polymer Size on the Effective Depletion Potential.** The effect of polymer size was explored theoretically as well. We chose the polymer reservoir packing fraction  $\eta_p^r$  such that the depletion attractive strength between smooth spheres was set at  $6 k_B T$  upon changing the polymer size. For the smallest polymers, the polymer reservoir fraction was 0.04, while the highest was 0.58. The latter polymer reservoir fraction lies in the semidilute regime, where one cannot assume that the polymers do not interact.<sup>30</sup> Figure 3 shows the attraction between two rough spheres covered with 250 small particles of diameter  $0.15\sigma_c$  for various polymer reservoir packing fractions  $\eta_p^r$ .

Figure 3 demonstrates that when the polymer has approximately the same size as the small particles used for the roughness, the attraction between rough particles is nearly as strong as between the smooth particles. However, the range of this attraction is longer:  $\sigma_p + \sigma_r$  (versus  $\sigma_p$  for two smooth particles). For smaller polymers, the attraction is suppressed until the potential is purely repulsive, in this case for  $\sigma_p \approx 0.05\sigma_c$ . In other words, smaller depletion agents are indeed more sensitive to particle roughness as they probe a larger part of the rough surface. Roughness is smoothed out by larger polymers. Notice also that the volume fraction of polymer required to obtain a reasonable attraction is much lower for the

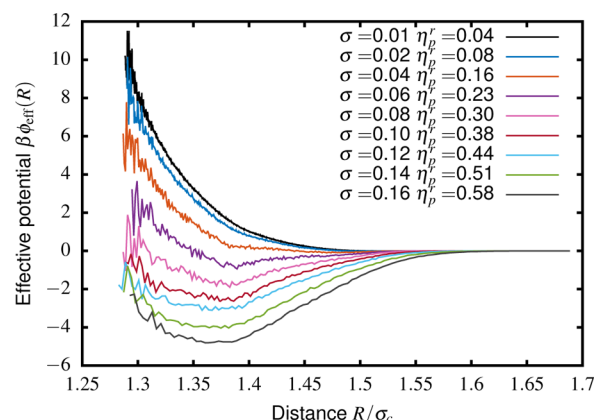


**Figure 3.** Effective depletion pair potential  $\beta\phi_{\text{eff}}^{\text{eff}}(R)$  as a function of center-to-center separation  $R$  between two rough spheres covered with 250 small spheres of  $0.15\sigma_c$ . The polymer diameter  $\sigma$  (given here as a fraction of  $\sigma_c$ ) and reservoir packing fraction  $\eta_p^r = z_p \sigma^3 \pi / 6$  are varied as labeled. The polymer reservoir packing fraction is chosen such that the attraction between smooth colloids is  $6 k_B T$ .

smaller polymers. A packing fraction well below the semidilute regime is satisfactory.

After submission of our paper, an extensive combined integral theory and Monte Carlo simulation approach was published investigating the effects of roughness on depletion forces as well.<sup>31</sup> One of the main conclusions in this recent paper is the same as ours: when surface roughness is on the same order as the size of the depletion agent, attractions between the rough particles are much reduced compared to smooth spheres and phase separation can be suppressed.

Closely related to polymer size, charge/steric stabilization also affect the effective depletion potential; an elaborate discussion on this point is in the SI.

#### Simulations: Effect of Ionic Strength during Particle Formation.

In the simulations, the random aggregation process leads to different appearances of roughness on the particle surface, depending on  $\kappa\sigma_c$  and the initial fraction of small colloids in the binary mixture. For low  $\kappa\sigma_c$ , the small particles are evenly distributed and very structured on the surface of the large particles, while for high  $\kappa\sigma_c$ , they are much more disordered. We chose  $\kappa\sigma_c = 10$ , since the resulting configurations showed the strongest resemblance to the synthesized particles. The final surface coverage of the simulated particles depends on the volume fraction of small particles in the simulated binary mixture. Figure 4a shows simulated colloids with various surface coverages. A surface coverage of 200 small particles was employed in all simulations of the experimental system, based on similarity in appearance and a similar number count of small particles on one hemisphere in Figure 5a (roughly 100 particles on the visible hemisphere).

#### Simulations: Prediction of the effective potential for the experimental system.

Experimental parameters such as polymer size were chosen based on the theoretical predictions drawn from the above simulation results. A pair potential was then also calculated based on the specific parameters in the experimental system, such as the diameters  $\sigma_o$ ,  $\sigma_r$ , and  $\sigma_c$ . The corresponding pair potentials for two smooth particles, two rough particles and a rough and a smooth particle are shown in Figure 4b. For  $\eta_p^r = 0.15$  the smooth particles have an attraction of approximately  $6k_B T$ , sufficient to be well inside the gel

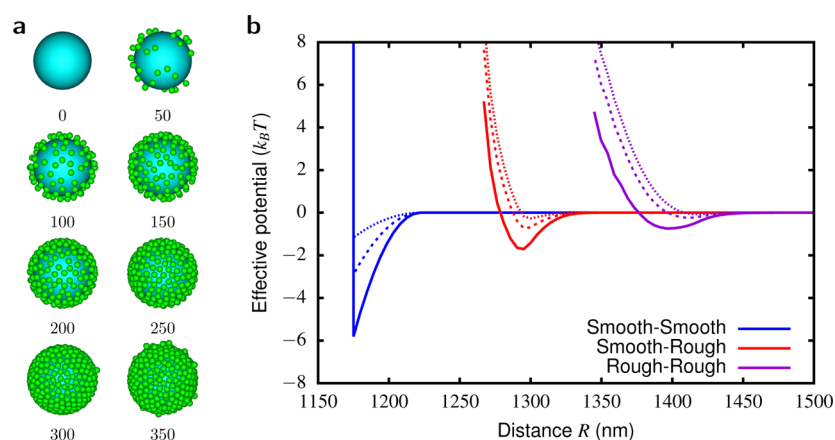


**Figure 4.** (a) Snapshots of generated rough particles, obtained as described in the section [Methods](#) with a screening length of  $\kappa\sigma = 10$ . (b) The effective pair potential  $\beta\phi^{\text{eff}}(r)$  as a function of center-to-center separation for the rough and smooth particles for parameters close to those used in the experiments:  $\sigma_c = 1175$  nm,  $\sigma_r = 122$  nm,  $\sigma_p = 46$  nm, and a coverage of 200 small particles per large particle. The solid, dashed, and dotted lines are for  $\eta_p^r = 0.15, 0.08,$  and  $0.03$  respectively.

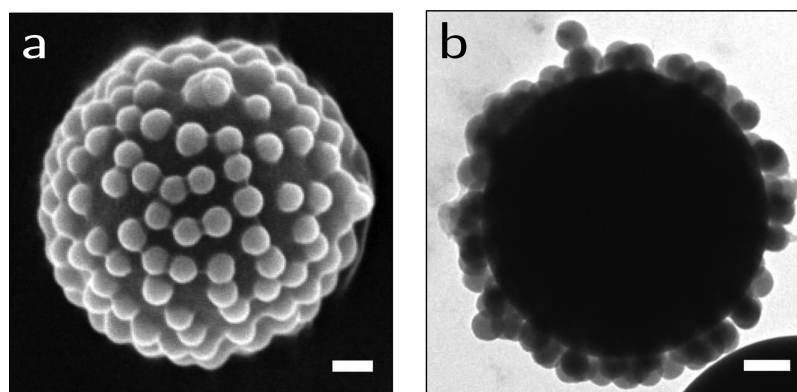


**Figure 5.** Micrographs of rough fluorescently labeled silica particles (core size  $\sigma = 1.18$   $\mu\text{m}$ , small sphere size 130 nm) imaged by (a) SEM and (b) TEM. Scale bars represent 200 nm. Additional SEM micrographs are in [Figure S5](#).

regime.<sup>32,33</sup> The rough particles on the other hand have a very weak attraction minimum on the order of  $k_B T$ , and will be able to escape from this attraction due to Brownian motion. A rough and a smooth particle have a slightly deeper attraction minimum of approximately  $2k_B T$ , not sufficient to phase separate.

**Experimental Results.** Transmission electron microscopy (TEM) and Scanning electron microscopy (SEM) images of the synthesized rough particles are shown in [Figure 5](#). The geometry of these particles displays an incomplete surface coverage, which according to the simulations is more effective in suppressing depletion interactions than a complete surface coverage.

The size of the smooth particles was carefully chosen in the following manner. The “size” of the rough particles was assumed to be  $\sigma_c + \sigma_r = 1.31$   $\mu\text{m}$  (i.e., the size of a sphere centered on the seed colloid through the centers of the adsorbed small particles). The smooth particles are slightly smaller: 1.24  $\mu\text{m}$ . Solely based on size, the depletion attraction between the smooth particles would be smaller than that between the rough particles, but the roughness reduces the depletion potential of the latter species. The polymer size was carefully chosen to be smaller than the size of the surface roughness (small particles), since the simulations had pointed out this is required for effective reduction of the depletion attraction: a larger polymer effectively smoothes the surface

roughness. In our case, the hydrodynamic radius of gyration of the polymer in this solution is  $23 \pm 1$  nm, which is less than half the radius of the small particles. Simultaneously, the double layer must be small compared to the surface roughness and the polymers, lest the double layer inhibit depletion attraction instead of the surface roughness. For this reason, the double layer was reduced by adding salt to the solvent. From the conductivity of a CHC stock solution (without polymer added), a Debye length of 41 nm was estimated using Walden’s rule. This Debye length equals  $0.32\sigma_r$ , and is on the order of the polymer diameter, hence we assume a moderate smoothing effect.

In dispersions without depletant, no clustering of either species was observed even after 2 days. We inferred that particles of both species are thermodynamically stable in this solvent. To establish the polymer concentrations at which the onset of the depletion interaction occurs, the fraction of particles sticking to the top wall of a capillary—30 min after turning the capillary upside down—was measured for various polymer concentrations. When the buoyant force of the particles exceeds the depletion attraction with the wall, all particles must fall to the bottom glass after turning. [Figure 6](#) shows the fraction of particles adhering to the top wall as a function of polymer concentration for both smooth and rough particles. The depletion attraction between two particles of one species—or even of different species—as smaller than the

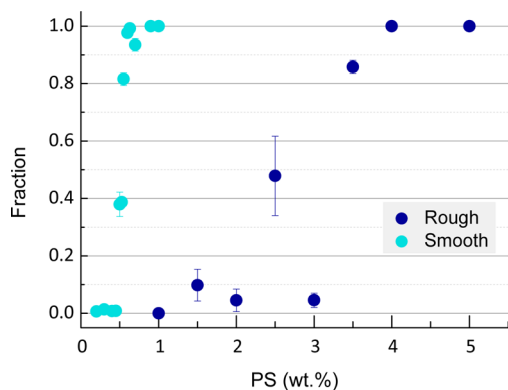


**Figure 6.** Sticking fraction of particles sticking to the top wall after turning a capillary, as a function of depletant PS concentration.

depletion attraction between a particle and a capillary wall, since the flat wall has no curvature or roughness and this implies a larger overlap volume. For smooth particles, the attraction to a wall equals roughly twice the attraction between two particles,<sup>9</sup> and we find a similar behavior for a rough particle and a flat wall (see SI). The smooth particles start to be attracted to the capillary wall at approximately 0.5 wt % depletant corresponding to  $3 k_B T$  adhesion, whereas the rough particles require at least 2.5 wt %. In other words, these measurements provide a lower limit of 1.0 wt % for the polymer concentration needed for gelation of the smooth particles, while the lower limit at which rough particles are expected to aggregate is expected to be roughly 5 times larger.

For a polymer concentration of 2 wt % PS (corresponding to a polymer packing fraction  $\eta \approx 0.154$ ), a sample of smooth particles (70 g/L) showed large clusters after 1 day in the rotating stage. In a sample of rough particles (70 g/L) with a polymer concentration of 2 wt % PS no such clustering was observed. Therefore, equal volumes of these dispersions were combined and a sample capillary was filled with this mixed dispersion. The sample was observed 5 h after preparation, which included sonication of the sample and leaving it horizontally. This sample contained large clusters of the smooth particles but nearly all rough particles were undergoing Brownian motion (see Figure 7 and the video in the SI).

The structure of the dispersion with 2 wt % polymer—shown in Figure 7—is in qualitative agreement with the

predictions in Figure 2. The large clusters in Figure 7a have an open, branched structure, indicating a strong depletion interaction between the smooth particles, which agrees with the deep attraction minimum ( $6 k_B T$ ) found in the theoretical calculation of the pair potential. The time-averaged Figure 7b shows that the smooth particles—trapped in clusters—did not move, whereas the rough particles have explored the space between the clusters through Brownian motion. Thus, we have found a depletant concentration for which the smooth particles spinodally demix, yet the rough particles can move freely. A few rough particles are sharply visible in the time averaged image as well, implying that those particles are trapped in the cluster. This trapping can be due to the potential minimum between rough and smooth particles, for the theoretical calculations show a minimum in the potential between rough and smooth particles.

In short, surface roughness was successfully used as a property to selectively immobilize (inhibit Brownian motion) in a mixture of two species of particles. Figure 4 shows the attraction minima for particle sizes and polymer packing fraction ( $\eta_p^* = 0.15$ ) close to those used in the experiments. We thus confirmed experimentally that the predicted large difference in attraction strength between smooth/smooth and rough/rough particle exists and can be exploited.

## CONCLUSIONS

We have computationally and experimentally investigated the extent to which a polymer induced depletion attraction can be reduced by roughness on the particle surface for similarly sized colloidal spheres. We found that it is possible to induce a sufficient difference in the rough/rough and rough/smooth depletion attraction strength on the one hand, and the smooth/smooth depletion attraction strength on the other hand. As a result, the latter particles gel, while the former remain completely mobile. As the depletion overlap volume for spheres is “least” optimal and thus a kind of limiting case, this finding is of importance for inducing specificity with respect to depletion-induced attraction for other particles shapes as well. We indicated how by simulations the effective interactions can be estimated. In addition, we provided a simple experimental procedure to gauge the interaction strengths by balancing depletion attractions with a flat wall against gravity. In future research, it would be interesting to see whether any

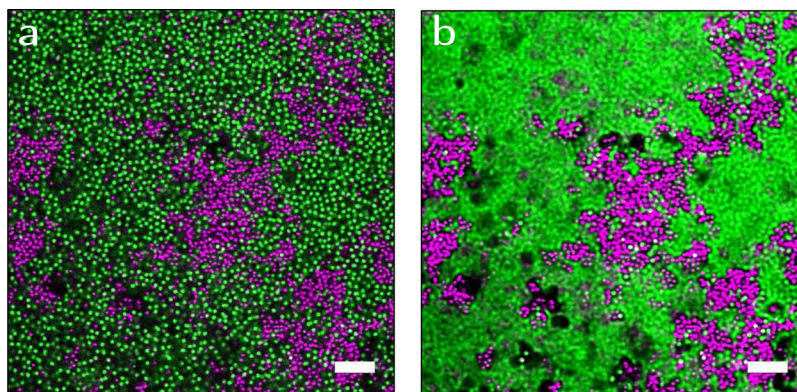


**Figure 7.** Confocal microscope images of a dispersion of smooth (purple) and rough (green) spheres. The sample contains 2 wt % PS and was imaged 5 h after preparation. The smooth spheres have aggregated into a cluster while the rough spheres can move freely. (a) Single snapshot of the dispersion. (b) Average over 60 frames. The time between successive images was 635 ms. Black spots are air bubbles moved to the field of view due to sonication. The scale bars denote 10  $\mu\text{m}$ .

ordered structures could be formed by carefully tuning the salt concentration in the dispersion.

## ■ ASSOCIATED CONTENT

### Supporting Information

The Supporting Information is available free of charge on the ACS Publications website at DOI: 10.1021/acs.langmuir.5b04001.

Experimental details, simulation details, SEM images, and additional references (PDF)

Supplementary video (AVI)

## ■ AUTHOR INFORMATION

### Corresponding Authors

\*E-mail: m.dijkstra@uu.nl (M.D.).

\*E-mail: a.vanblaaderen@uu.nl (A.v.B.).

### Author Contributions

M.H. performed the computer simulations, while M.K. performed the experiments. C.M.v.K. synthesized the rough silica particles. D.J.K. and W.K.K. shared essential knowledge on depletion interactions in systems of rough and smooth particles. A.v.B. designed and supervised the experimental research, and M.D. the computational research. The manuscript was cowritten by M.K. and M.H. and discussed by all authors.

### Notes

The authors declare no competing financial interest.

## ■ ACKNOWLEDGMENTS

We thank A.F. Demirörs for synthesis of the silica particles used as the smooth species and J.C.P. Stiefelhagen for synthesis of the PHSA. M.K. acknowledges funding from the Netherlands Organisation for Scientific Research (NWO) (project number 700.58.025). Additionally, funding was received from the European Research Council under the European Unions Seventh Framework Programme (FP/2007-2013)/ERC Grant Agreement no. 291667.

## ■ REFERENCES

- (1) van Blaaderen, A. Materials Science: Colloids get Complex. *Nature* **2006**, *439*, 545–546.
- (2) Glotzer, S. C.; Solomon, M. J. Anisotropy of Building Blocks and their Assembly into Complex Structures. *Nat. Mater.* **2007**, *6*, 557–562.
- (3) Yang, S.-M.; Kim, S.-H.; Lim, J.-M.; Yi, G.-R. Synthesis and Assembly of Structured Colloidal Particles. *J. Mater. Chem.* **2008**, *18*, 2177–2190.
- (4) Sacanna, S.; Pine, D. J. Shape-Anisotropic Colloids: Building Blocks for Complex Assemblies. *Curr. Opin. Colloid Interface Sci.* **2011**, *16*, 96–105.
- (5) Asakura, S.; Oosawa, F. Interaction between Particles Suspended in Solutions of Macromolecules. *J. Polym. Sci.* **1958**, *33*, 183–192.
- (6) Jenkins, P.; Snowden, M. Depletion Flocculation in Colloidal Dispersions. *Adv. Colloid Interface Sci.* **1996**, *68*, 57–96.
- (7) Lekkerkerker, H. N. W.; Poon, W. C.-K.; Pusey, P. N.; Stroobants, A.; Warren, P. B. Phase Behaviour of Colloid + Polymer Mixtures. *Europhys. Lett.* **1992**, *20*, 559–564.
- (8) Tuinier, R.; Rieger, J.; de Kruijff, C. G. Depletion-Induced Phase Separation in Colloid-Polymer Mixtures. *Adv. Colloid Interface Sci.* **2003**, *103*, 1–31.
- (9) Lekkerkerker, H. N. W.; Tuinier, R. *Colloids and the Depletion Interaction*; Springer: Netherlands, 2011.
- (10) Jamie, E. A. G.; Dullens, R. P. A.; Aarts, D. G. A. L. Tuning the Demixing of Colloid-Polymer Systems through the Dispersing Solvent. *J. Phys.: Condens. Matter* **2011**, *23*, 194115.

(11) Badaire, S.; Cottin-Bizonne, C.; Stroock, A. D. Experimental Investigation of Selective Colloidal Interactions Controlled by Shape, Surface Roughness, and Steric Layers. *Langmuir* **2008**, *24*, 11451–11463.

(12) Zhao, K.; Mason, T. G. Directing Colloidal Self-Assembly through Roughness-Controlled Depletion Attractions. *Phys. Rev. Lett.* **2007**, *99*, 268301.

(13) Dinsmore, A. D.; Yodh, A. G. Entropic Confinement of Colloidal Spheres in Corners on Silicon Substrates. *Langmuir* **1999**, *15*, 314–316.

(14) Sacanna, S.; Irvine, W. T. M.; Chaikin, P. M.; Pine, D. J. Lock and Key Colloids. *Nature* **2010**, *464*, 575–578.

(15) Kraft, D. J.; Ni, R.; Smalenburg, F.; Hermes, M.; Yoon, K.; Weitz, D. A.; van Blaaderen, A.; Groenewold, J.; Dijkstra, M.; Kegels, W. K. Surface roughness directed self-assembly of patchy particles into colloidal micelles. *Proc. Natl. Acad. Sci. U. S. A.* **2012**, *109*, 10787–10792.

(16) Rossi, L.; Soni, V.; Ashton, D. J.; Pine, D. J.; Philipse, A. P.; Chaikin, P. M.; Dijkstra, M.; Sacanna, S.; Irvine, W. T. M. Shape-sensitive crystallization in colloidal superball fluids. *Proc. Natl. Acad. Sci. U. S. A.* **2015**, *112*, 5286–5290.

(17) Harley, S.; Thompson, D. W.; Vincent, B. The Adsorption of Small Particles onto Larger Particles of Opposite Charge: Direct Electron Microscope Studies. *Colloids Surf.* **1992**, *62*, 163–176.

(18) Dijkstra, M.; van Roij, R.; Evans, R. Phase Behavior and Structure of Binary Hard-Sphere Mixtures. *Phys. Rev. Lett.* **1998**, *81*, 2268–2271.

(19) Dijkstra, M.; van Roij, R.; Evans, R. Direct Simulation of the Phase Behavior of Binary Hard-Sphere Mixtures: Test of the Depletion Potential Description. *Phys. Rev. Lett.* **1999**, *82*, 117–120.

(20) Dijkstra, M.; van Roij, R.; Evans, R. Phase Diagram of Highly Asymmetric Binary Hard-Sphere Mixtures. *Phys. Rev. E: Stat. Phys., Plasmas, Fluids, Relat. Interdiscip. Top.* **1999**, *59*, 5744–5771.

(21) Dijkstra, M.; Brader, J. M.; Evans, R. Phase Behaviour and Structure of Model Colloid-Polymer Mixtures. *J. Phys.: Condens. Matter* **1999**, *11*, 10079.

(22) Bolhuis, P. G.; Louis, A. A.; Hansen, J.-P. Influence of Polymer-Excluded Volume on the Phase-Behavior of Colloid-Polymer Mixtures. *Phys. Rev. Lett.* **2002**, *89*, 128302.

(23) Decher, G. Fuzzy Nanoassemblies: Toward Layered Polymeric Multicomposites. *Science* **1997**, *277*, 1232–1237.

(24) Lvov, Y.; Decher, G.; Moehwald, H. Assembly, Structural Characterization, and Thermal Behavior of Layer-by-Layer Deposited Ultrathin Films of Poly(Vinyl Sulfate) and Poly(Allylamine). *Langmuir* **1993**, *9*, 481–486.

(25) Decher, G.; Schlenoff, J. B. *Multilayer Thin Films: Sequential Assembly of Nanocomposite Materials*; Wiley-VCH Verlag GmbH & Co: Weinheim, 2012.

(26) Schmitt, J.; Decher, G.; Dressick, W. J.; Brandow, S. L.; Geer, R. E.; Shashidhar, R.; Calvert, J. M. Metal Nanoparticle/Polymer Superlattice Films: Fabrication and Control of Layer Structure. *Adv. Mater.* **1997**, *9*, 61–65.

(27) Russel, W. B.; Saville, D. A.; Schowalter, W. R. *Colloidal Dispersions*; Cambridge University Press: Cambridge, 1989.

(28) El Masri, D.; Vissers, T.; Badaire, S.; Stiefelhagen, J. C. P.; Vutukuri, H. R.; Helfferich, P.; Zhang, T. H.; Kegels, W. K.; Imhof, A.; van Blaaderen, A. A Qualitative Confocal Microscopy Study on a Range of Colloidal Processes by Simulating Microgravity Conditions through Slow rotations. *Soft Matter* **2012**, *8*, 6979–6990.

(29) Crocker, J. C.; Grier, D. G.; Weeks, E. R. <http://www.physics.emory.edu/faculty/weeks/idl/>.

(30) de Gennes, P. G. *Scaling Concepts in Polymer Physics*; Cornell University Press: Cornell, 1979.

(31) Banerjee, D.; Yang, J.; Schweizer, K. S. Entropic Depletion in Colloidal Suspensions and Polymer Liquids: Role of Nanoparticle Surface Topography. *Soft Matter* **2015**, *11*, 9086–9098.

(32) Miller, M. A.; Frenkel, D. Phase Diagram of the Adhesive Hard Sphere Fluid. *J. Chem. Phys.* **2004**, *121*, 535–545.

(33) Lu, P. J.; Zaccarelli, E.; Ciulla, F.; Schofield, A. B.; Sciortino, F.; Weitz, D. A. Gelation of Particles with Short-Range Attraction. *Nature* **2008**, *453*, 499–503.